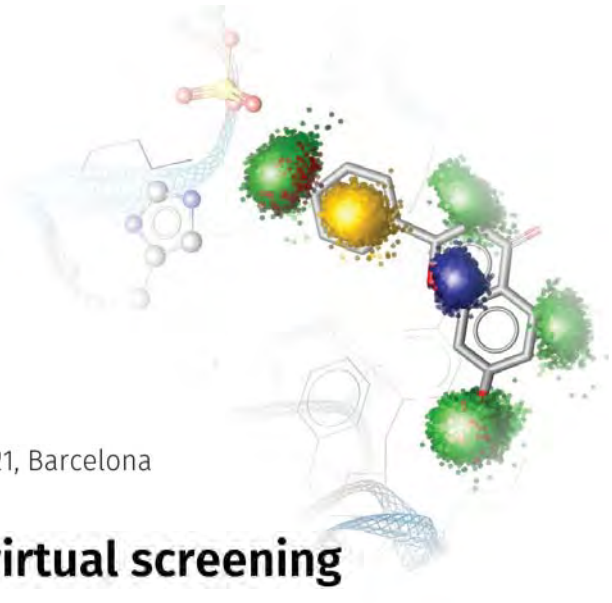

BIGCHEM BCN 2017, April 19-21, Barcelona

3D pharmacophores for virtual screening

Gerhard Wolber
gerhard.wolber@fu-berlin.de
Institute of Pharmacy - Pharmaceutical Chemistry – Computer-Aided Drug Design
Freie Universität Berlin

Exploring protein-ligand binding ...

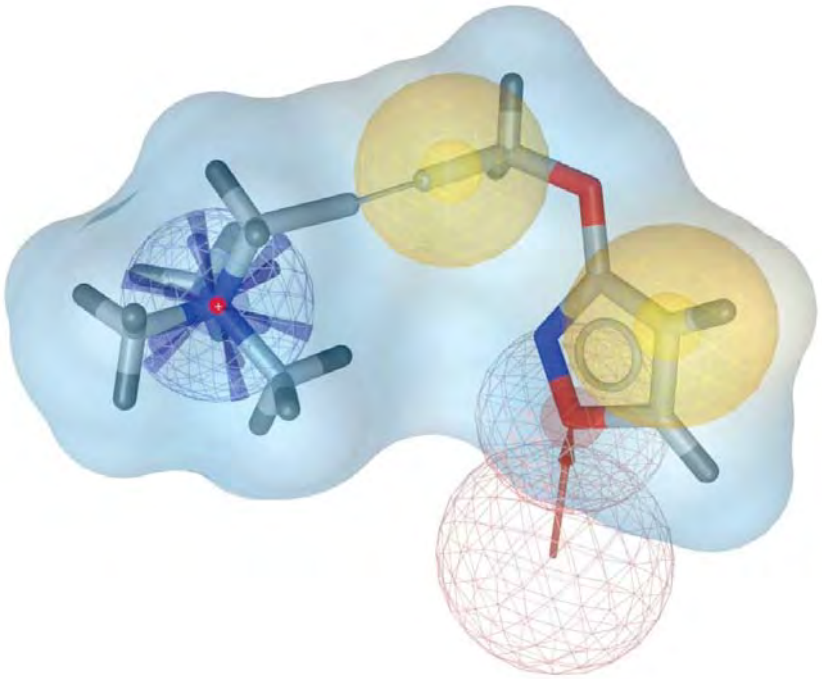

3D pharmacophores for virtual screening

3D pharmacophores: applications

- Virtual screening
- Lead optimization & SAR
- Understanding protein function
- Design of ligands for new pockets

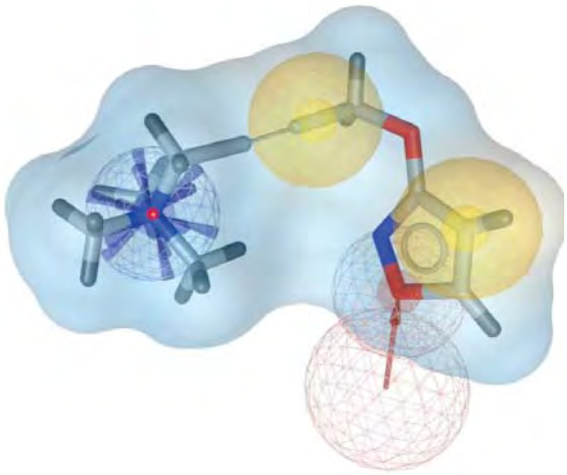

Algorithms & Big data

- Implementation matters! A few words on 3D alignment
- Dynophores: Bridging theoretical chemistry and drug design

Why 3D Pharmacophores?

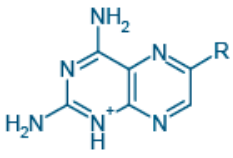

Methotrexate

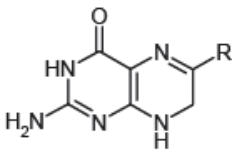

Dihydrofolate

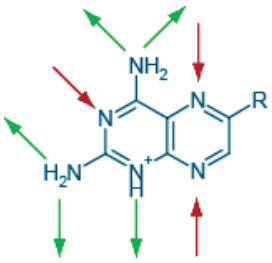

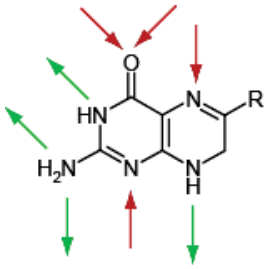

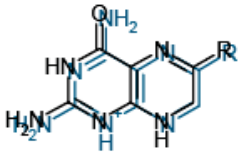

Wrong

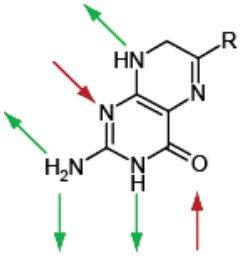

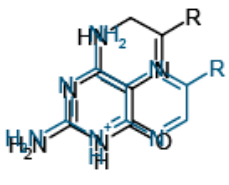

Correct

Böhm, Klebe, Kubinyi: Wirkstoffdesign (1999) p. 320f

Why 3D Pharmacophores?

Characteristics & advantages:

- Universal (scaffold-hopping)
- Computationally efficient
- 'Traditional way of thinking' in medicinal chemistry

Application areas:

- Virtual Screening
- Hit/lead optimization & SAR
- Understanding protein function
- Design ligands for new pockets

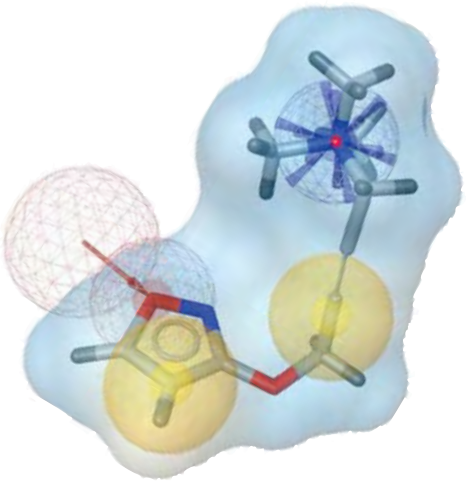

Virtual Screening: Peroxisome-Proliferator Activated Receptor Gamma (PPARγ)

Virtual Screening
Hit/lead optimization & SAR
Understanding protein function
Design ligands for new pockets

New PPARγ partial agonists (structure-based)
89k screened
10 virtual hits selected
5 are partial agonists (bind PPARγ, do not stimulate adipogenesis & enhance glucose uptake)

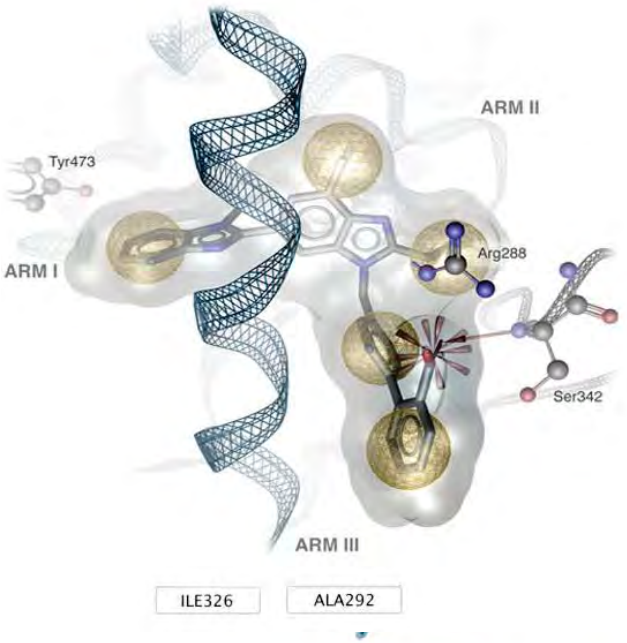

[1] Identification of PPARγ agonists from natural sources using different *in silico* approaches, *Planta Med*, 181(06):488-494, **2015**
[2] Identification of natural PPARγ partial agonists: Virtual screening & in vitro validation. *PLoS ONE 7*: e50816, **2012**
[3] Characterization of New PPARg Agonists: Benzimidazole Derivatives. *Bioorg. Med. Chem.*, 18(16): 5885-5895, **2010**
[4] Computer-aided discovery & mechanistic characterisation of neolignan activators of PPARg. *Mol. Pharm.*, 77(4): 559-566. **2010**

Novel Inhibitors of 17β-HSD 3 and 5

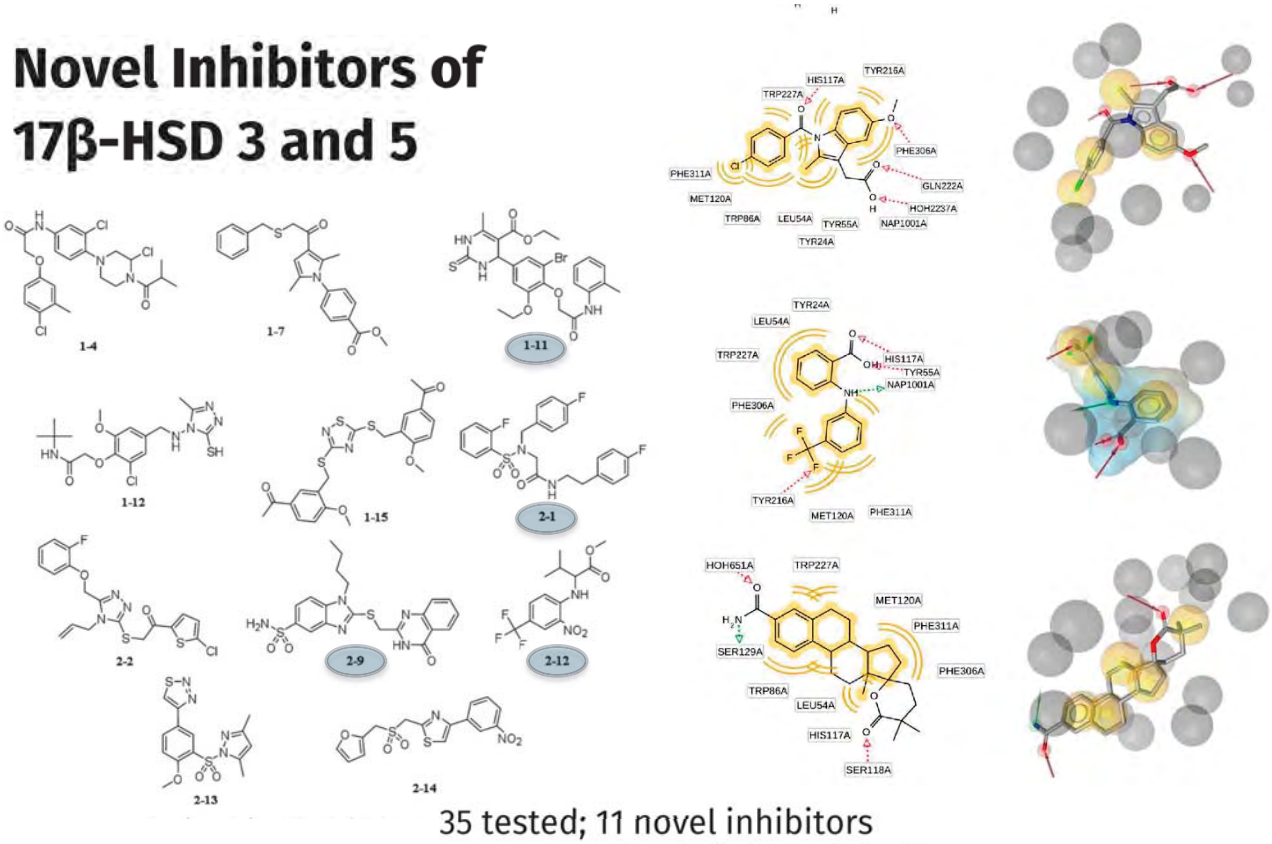

35 tested; 11 novel inhibitors
1-12, 2-1, 2-12 ~ 1µM, 2-9 ~ 0.3 µM

[1] Identification of chemically diverse, novel inhibitors of 17 beta-hydroxysteroid dehydrogenase type 3 and 5 by pharmacophore-based virtual screening, *J Steroid Biochem*, 125(1-2):148-161, 2011

[2] The UV-filter benzophenone-1 inhibits 17 beta-hydroxysteroid dehydrogenase type 3: Virtual screening as a strategy to identify potential endocrine disrupting chemicals, *Biochem Pharmacol*, 79(8):1189-1199, 2010.

Screening for Unwanted Effects: Sulfotransferase 1E1

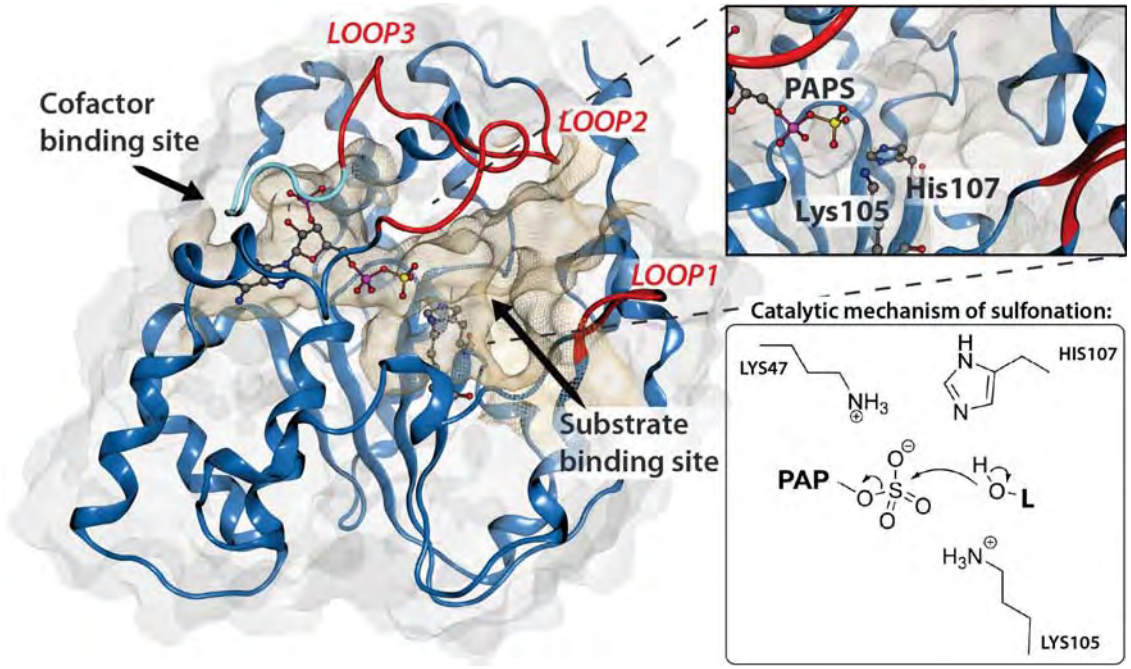

[1] C. Rakers, F. Schumacher, W. Meinl, H. Glatt, B. Kleuser, and G. Wolber. In silico prediction of human sulfotransferase 1E1 activity guided by pharmacophores from molecular dynamics simulations, *J Biol Chem*, 291(1):58-71, **2016**.

Screening for Unwanted Effects: Sulfotransferase 1E1

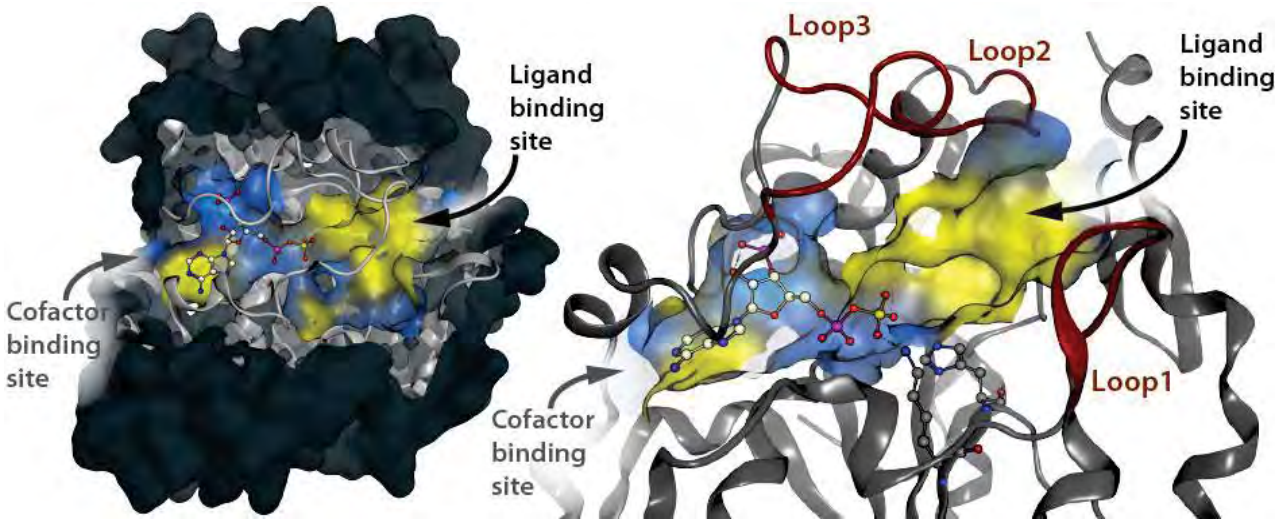

[1] C. Rakers, F. Schumacher, W. Meinl, H. Glatt, B. Kleuser, and G. Wolber. In silico prediction of human sulfotransferase 1E1 activity guided by pharmacophores from molecular dynamics simulations, *J Biol Chem*, 291(1):58-71, **2016**.

Screening for Unwanted Effects: Sulfotransferase 1E1

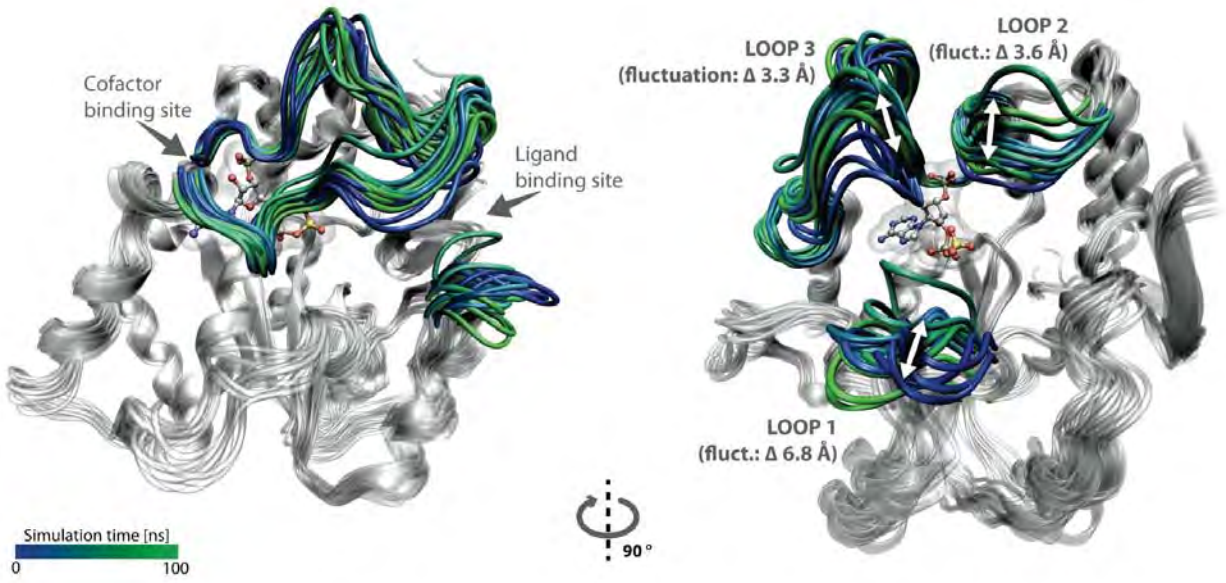

[1] C. Rakers, F. Schumacher, W. Meinl, H. Glatt, B. Kleuser, and G. Wolber. In silico prediction of human sulfotransferase 1E1 activity guided by pharmacophores from molecular dynamics simulations, *J Biol Chem*, 291(1):58-71, **2016**.

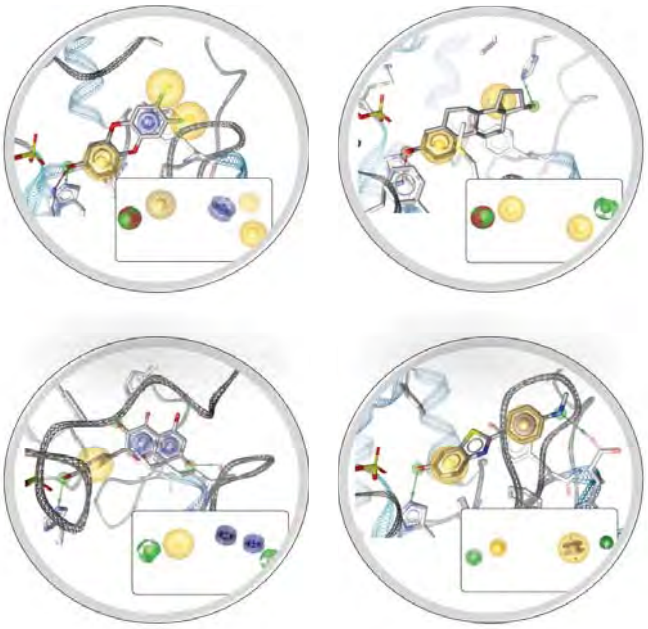

1. 8 different pharmacophores developed for classification: selected from molecular dynamics according to fit of ligands
2. Machine learning on applied on pharmacophore fit as descriptor

C. Rakers, F. Schumacher, W. Meinl, H. Glatt, B. Kleuser, and G. Wolber. In silico prediction of human sulfotransferase 1E1 activity guided by pharmacophores from molecular dynamics simulations, *J Biol Chem*, 291(1):58-71, **2016**.

Pharmacophore Application: SULT1E1

Virtual Screening
Hit/lead optimization & SAR
Understanding protein function
Design ligands for new pockets

Sulfotransferase 1E1 (structure-based)
Screened Drugbank (6500 drugs)
24 known ligands (35%)
From the remaining 44: 9 representative purchased and tested, all active and classified

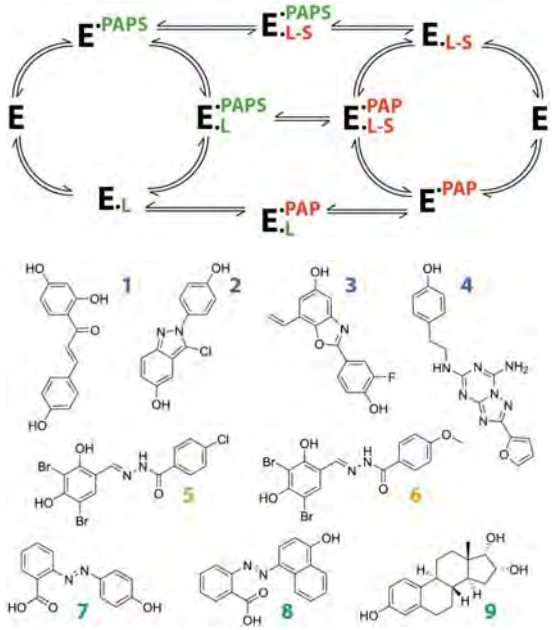

Concentration-dependent (CDL) - Inhibitor - Substrate

[1] C. Rakers, F. Schumacher, W. Meinl, H. Glatt, B. Kleuser, and G. Wolber. In silico prediction of human sulfotransferase 1E1 activity guided by pharmacophores from molecular dynamics simulations, *J Biol Chem*, 291(1):58-71, **2016**.

Pharmacophore Application: SULT1E1

Virtual Screening
Hit/lead optimization & SAR
Understanding protein function
Design ligands for new pockets

Sulfotransferase 1E1 (structure-based)
Screened Drugbank (6500 drugs)
24 known ligands (35%)
From the remaining 44: 9 representative purchased and tested, all active and classified correctly

	SULT1E1	FabZ*	Sirtuin 1
5	**IC_{50}=0.31 µM** (± 0.05)	IC_{50}=1.52µM (± 0.19)	$EC_{1.5}$=7.0µM
6	**IC_{50}=0.23 µM** (± 0.05)	IC_{50}=9.92 µM (± 0.59)	-

*β-Hydroxyacyl-Acyl Carrier Protein Dehydratase (FabZ) of Helicobacter pylori (He et al. *J. Med. Chem.*, 2009, 52 (8), pp 2465–2481)

[1] C. Rakers, F. Schumacher, W. Meinl, H. Glatt, B. Kleuser, and G. Wolber. In silico prediction of human sulfotransferase 1E1 activity guided by pharmacophores from molecular dynamics simulations, *J Biol Chem*, 291(1):58-71, **2016**.

Ligands for Phosphatases: PTP1B

Virtual Screening
Hit/lead optimization & SAR
Understanding protein function
Design ligands for new pockets

PTP1B inhibitor optimization (structure-based)
Compound optimization
Rationalization of SAR
Synthesis support

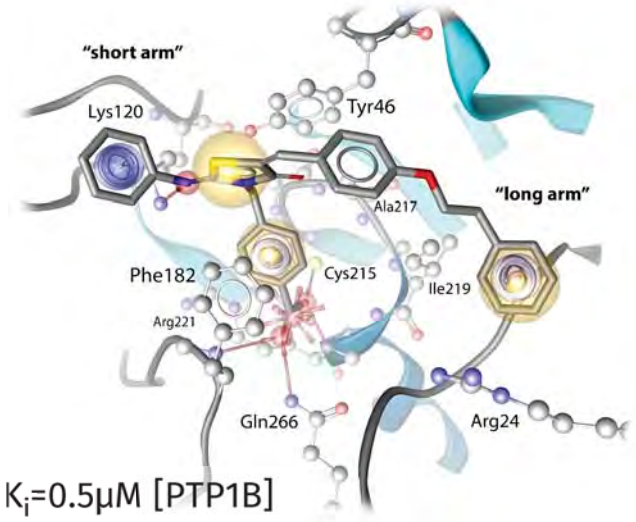

K_i=0.5µM [PTP1B]

[1] Selective inhibitors of the protein tyrosine phosphatase SHP2 block cellular motility and growth of cancer cells in-vitro and in-vivo, *ChemMedChem*, 10(5):815-826, **2015**
[2] Synthesis, biological activity and structure-activity relationships of new benzoic acid-based protein tyrosine phosphatase inhibitors endowed with insulinomimetic effects in mouse C2C12 skeletal muscle cells, *Eur J Med Chem*, 71:112-127, **2014**
[3] New 4-[(5-arylidene-2-arylimino-4-oxo-3-thiazolidinyl)methyl]benzoic acids active as protein tyrosine phosphatase inhibitors endowed with insulinomimetic effect on mouse C2C12 skeletal muscle cells, *Eur J Med Chem*, 50:332-343, **2012**

Pharmacophore Application: Phenylalanine Hydroxylase (PAH)

Virtual Screening
Hit/lead optimization & SAR
Understanding protein function
Design ligands for new pockets

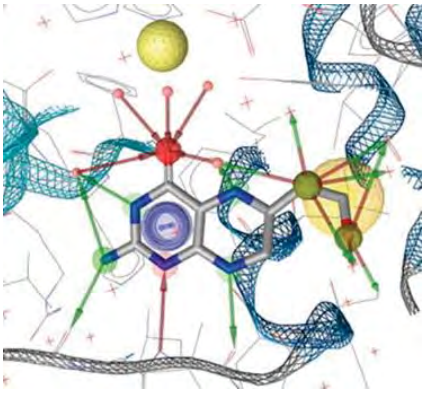

New PAH ligands as pharmacological chaperones (structure-based)

BH4-analogs
indirect water interactions
supported by SPR
250k screened: 85 selected, 6 restore enzyme activity

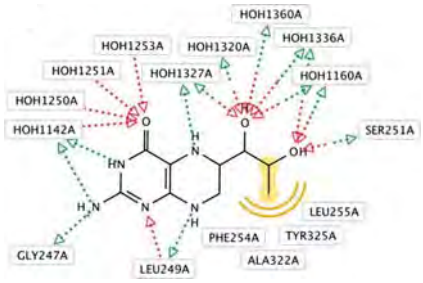

[1] Novel pharmacological chaperones that correct phenylketonuria in mice. Hum. Mol. Genet. 21(8):1877-1887, **2012**

Understanding Protein Function: G-Protein Coupled Receptors

Virtual Screening
Hit/lead optimization & SAR
Understanding protein function
Design ligands for new pockets

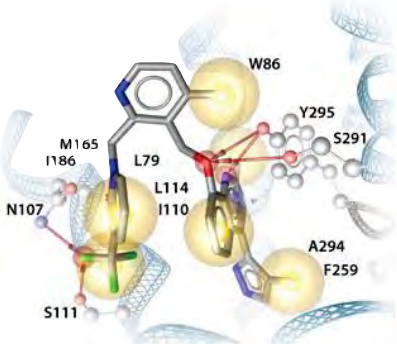

Bradykinin B2 receptor function (structure-based)

Homology modeling & dynamics
Ionic lock explained
rationalized new lead structures

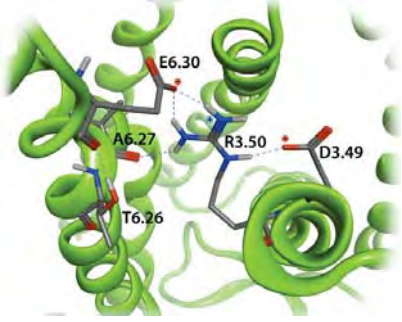

[1] J. Leschner, G. Wennerberg, J. Feierler, M. Bermudez, B. Welte, I. Kalatskaya, G. Wolber, and A. Faussner. nterruption of the ionic lock in the bradykinin B2 receptor results in constitutive internalization and turns antagonists into strong agonists. *J. Pharmacol. Exp. Ther.*, 344(1):85-95, **2012**
[2] A. Faussner, S. Schussler, J. Feierler, M. Bermudez, J. Pfeifer, K. Schnatbaum, T. Tradler, M. Jochum, G. Wolber, and C. Gibson. Binding characteristics of [3H]-JSM10292: a new cell membrane-permeant non-peptide bradykinin B2 receptor antagonist, *Br J Pharmacol*, 1167(4):839-853, **2012**
[3] Structure vs. function - the impact of computational methods on the discovery of specific GPCR-ligands, *Bioorg Med Chem*, 14(15): 3907-3912, **2015**

G-Protein-Coupled Receptors: Muscarinic Acetylcholine Receptor

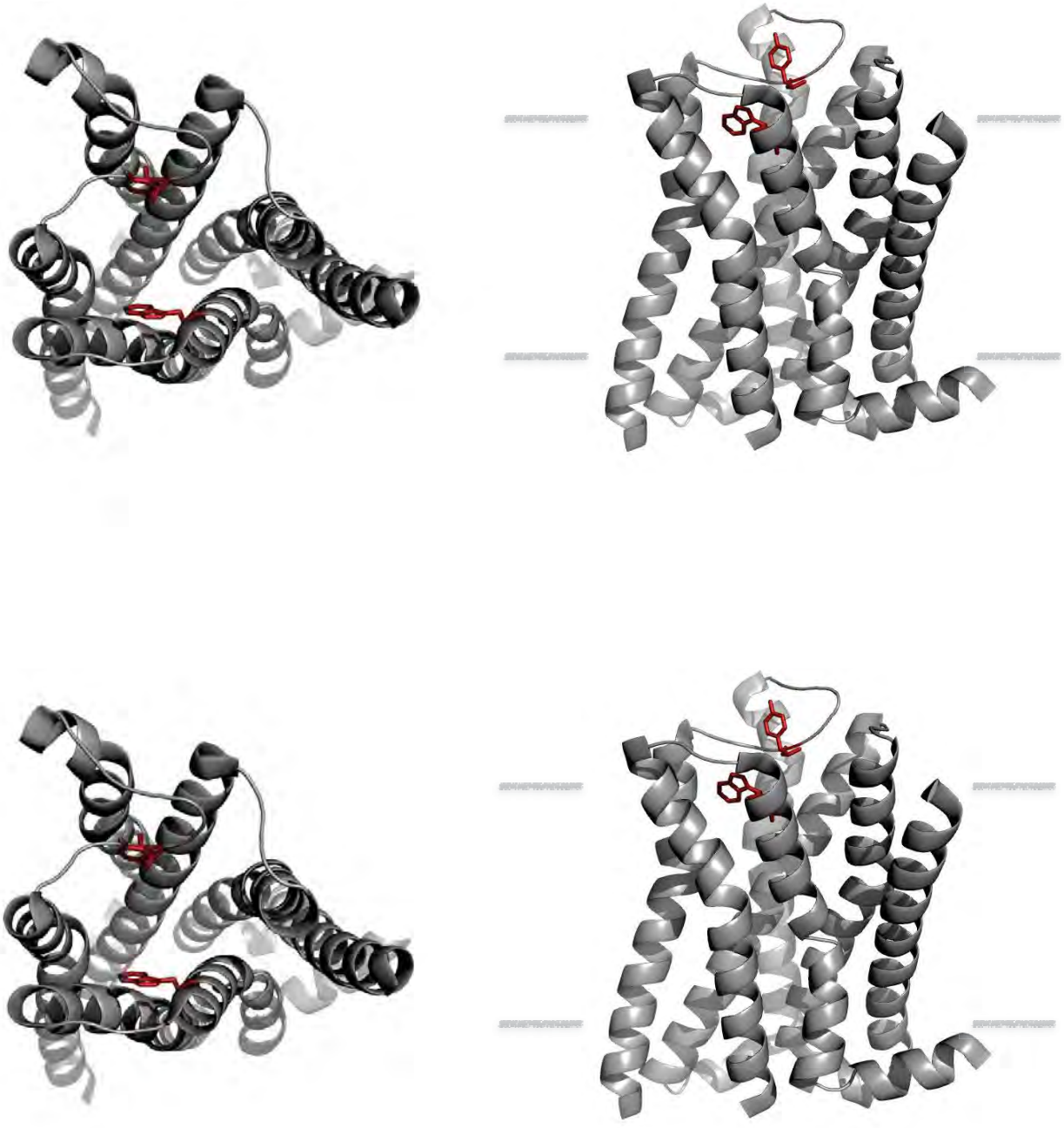

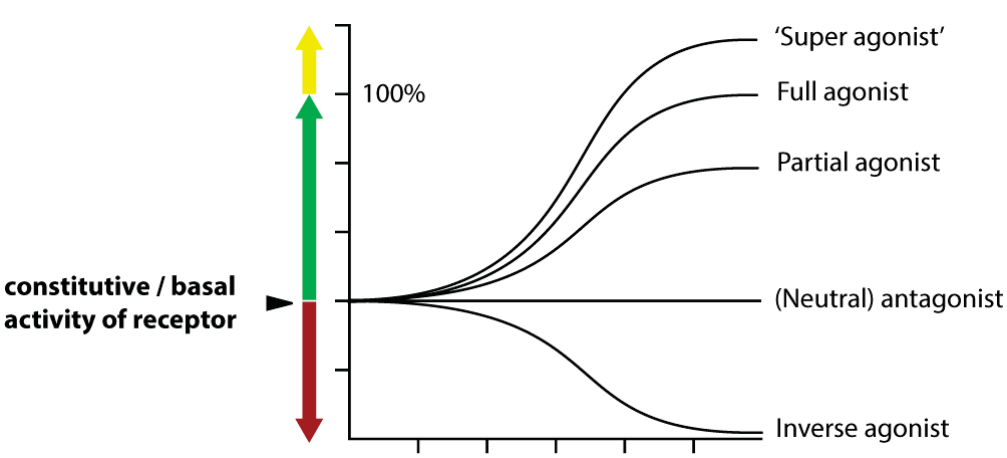

Which G-Protein?

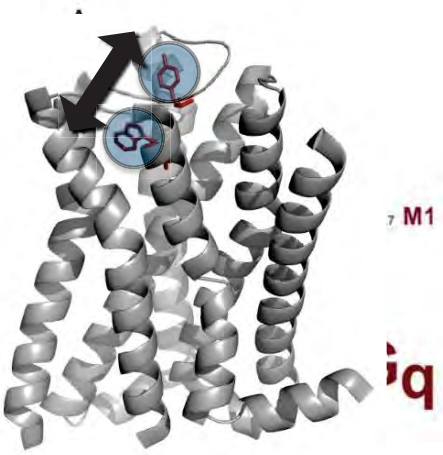

G_i coupling is linked to a larger conformational ensemble

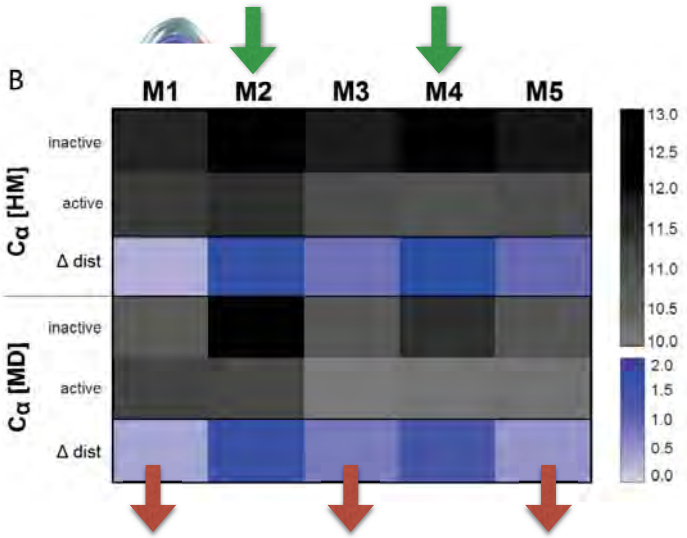

G_q coupling only occurs within a tightly restricted, specific conformational space

[1] M. Bermudez, C. Rakers, and G. Wolber. Structural Characteristics of the Allosteric Binding Site Represent a Key to Subtype Selective Modulators of Muscarinic Acetylcholine Receptors , Mol. Inf., 34: 526–53, **2015**

M2 Receptor: Orthosteric Ligands

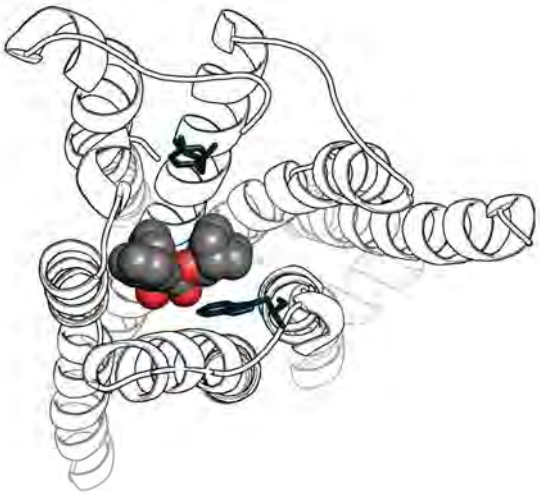

3UON with inverse Agonist QNB

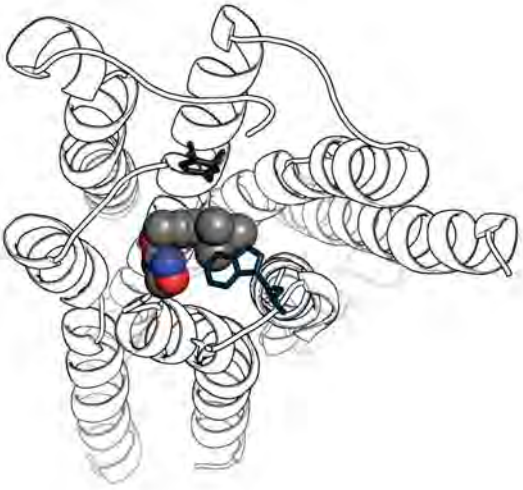

4MQS with (Super)Agonist Iperoxo

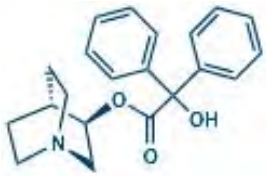

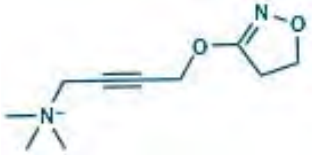

Selective Dualsteric M2 Ligands

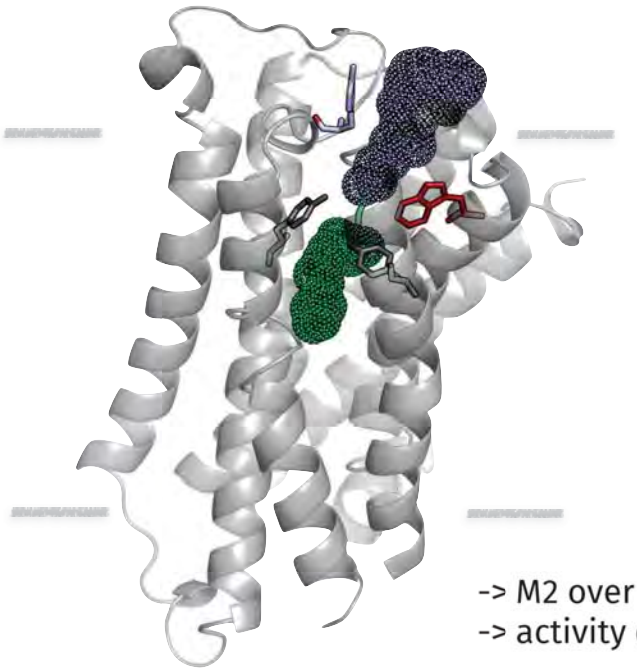

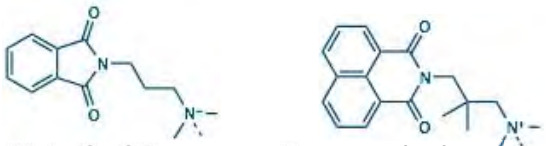

Phtalimide-based

Naphtalimide-based

+Linker (6C)

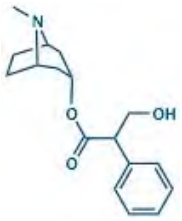

Atropin

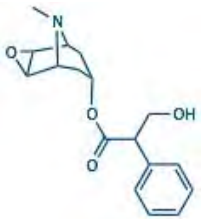

Scopolamin

-> M2 over M5 selectivity could be established
-> activity comparable to orthosteric inverse agonists

[1] J. Schmitz, D. van der Mey, M. Bermudez, J. Klöckner, R. Schrage, E. Kostenis, C. Tränkle, G. Wolber, K. Mohr, and U. Holzgrabe. Dualsteric muscarinic antagonists - orthosteric binding pose controls allosteric subtype-selectivity. J. Med. Chem. 57:6739-6750, **2014**

[2] Ligand Binding Ensembles Determine Graded Agonist Efficacies at a G Protein-coupled Receptor. *J Biol Chem* 291: 16375-16389, **2016**

3D Pharmacophores Explain Selectivity of Dualsteric Ligands

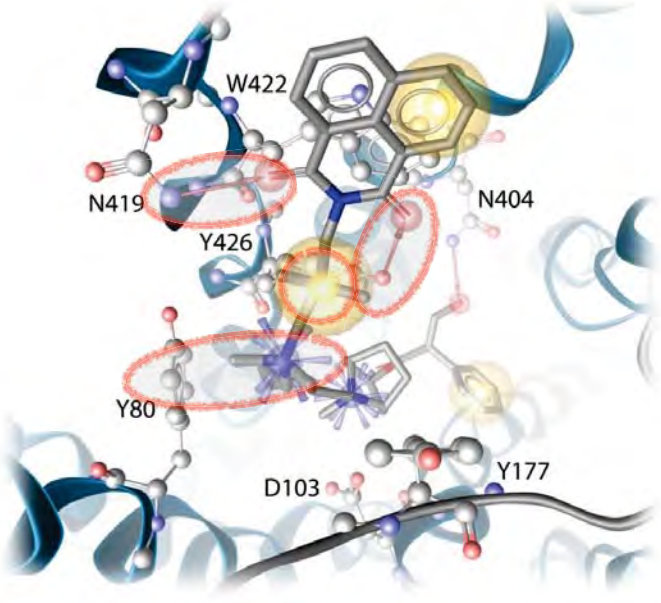

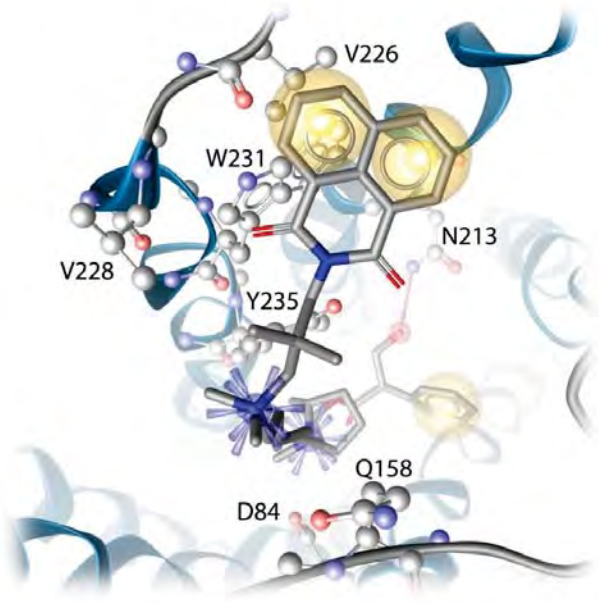

Atr-6-naph is selective (~10 fold) for the M2 receptor (left) over the M5 receptor (right)

Selective Dualsteric M2 Ligands

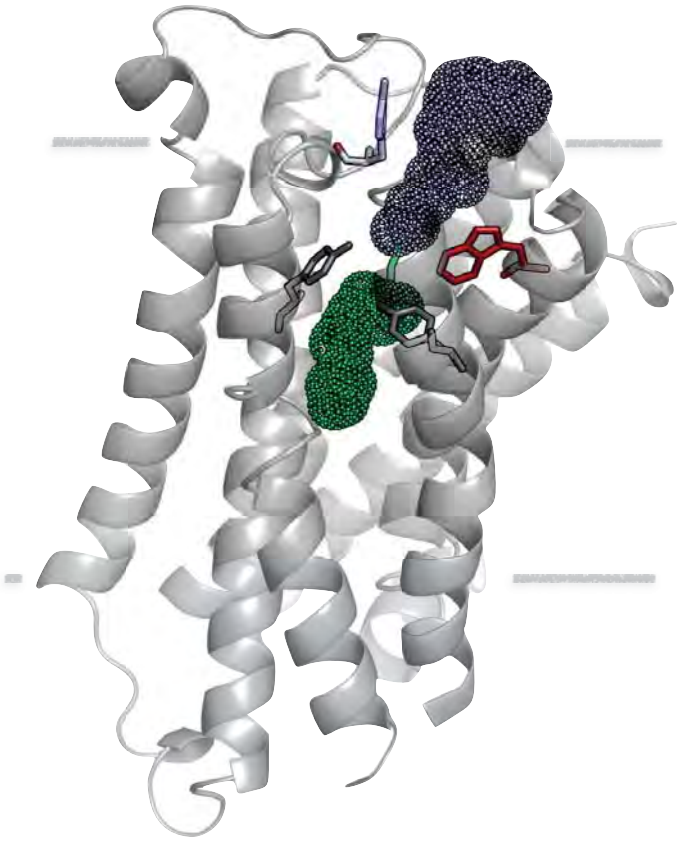

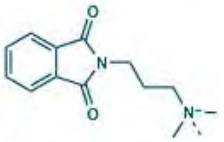

Phtalimide-based

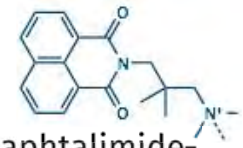

Naphtalimide-based

+Linker (6-8C)

Iperoxo

-> M2 over M5 selectivity
-> agonist hybrids restrict conformation
-> biased signalling ("partial agonism")

Agonist Hybrids

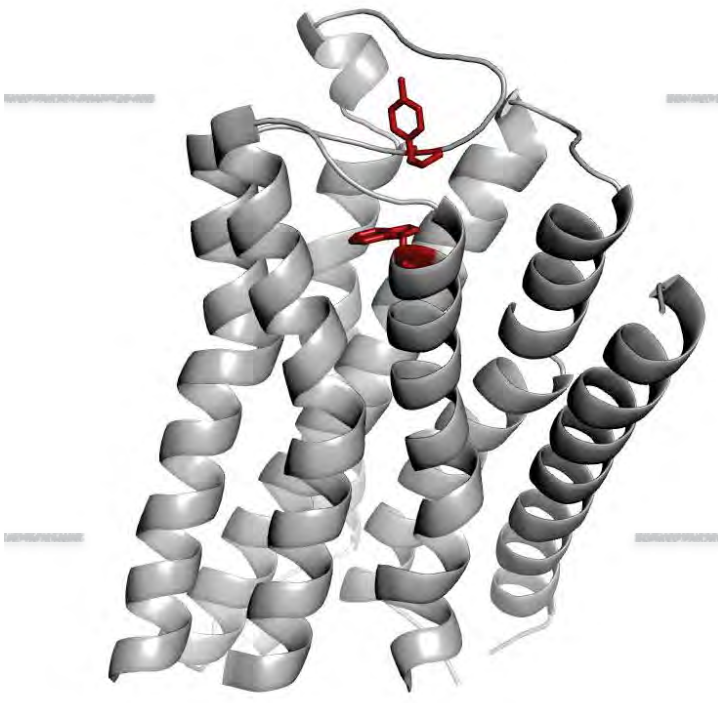

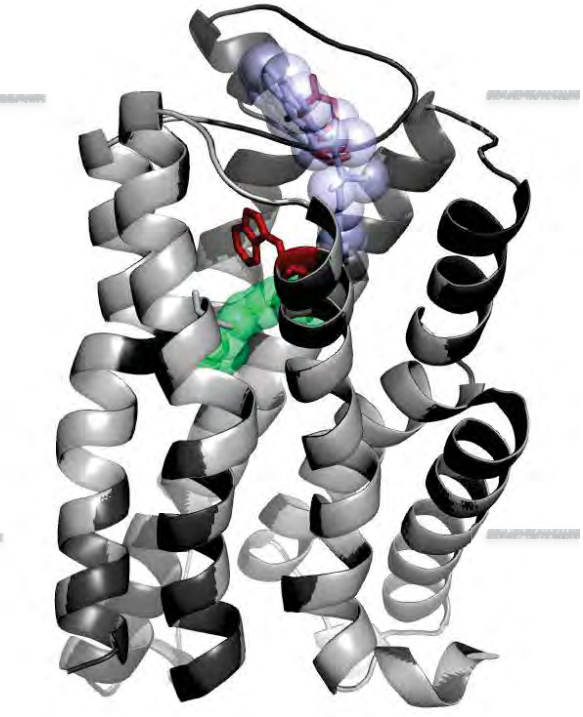

Agonist hybrids restrict conformation -> biased signalling ("G_i bias")

Dynophore analysis to compare binding behavior

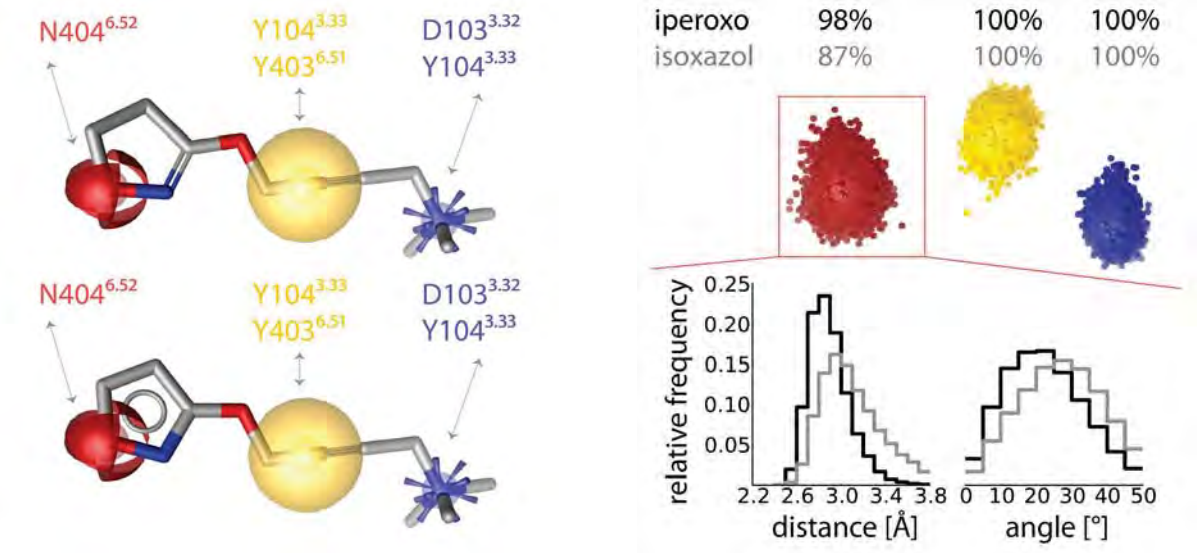

[1] Ligand Binding Ensembles Determine Graded Agonist Efficacies at a G Protein-coupled Receptor. *J Biol Chem* 291: 16375-16389, 2016

Dynophore analysis to compare binding behavior

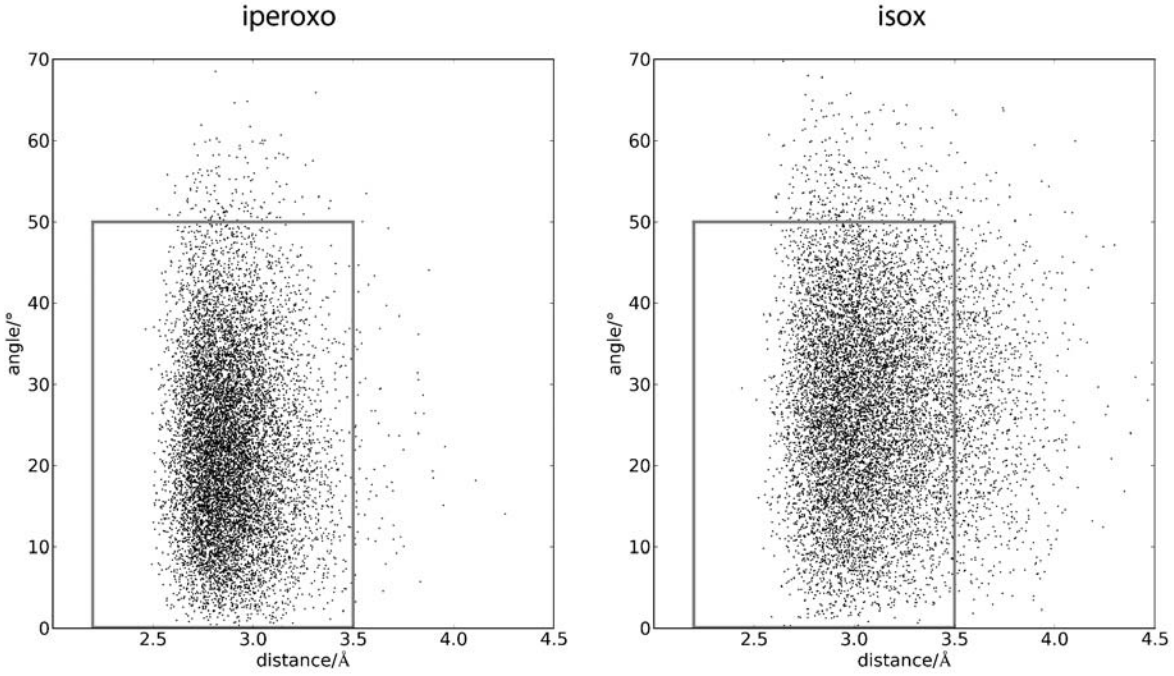

[1] Ligand Binding Ensembles Determine Graded Agonist Efficacies at a G Protein-coupled Receptor. *J Biol Chem* 291: 16375-16389, 2016

Toll-Like Receptor (TLR2)

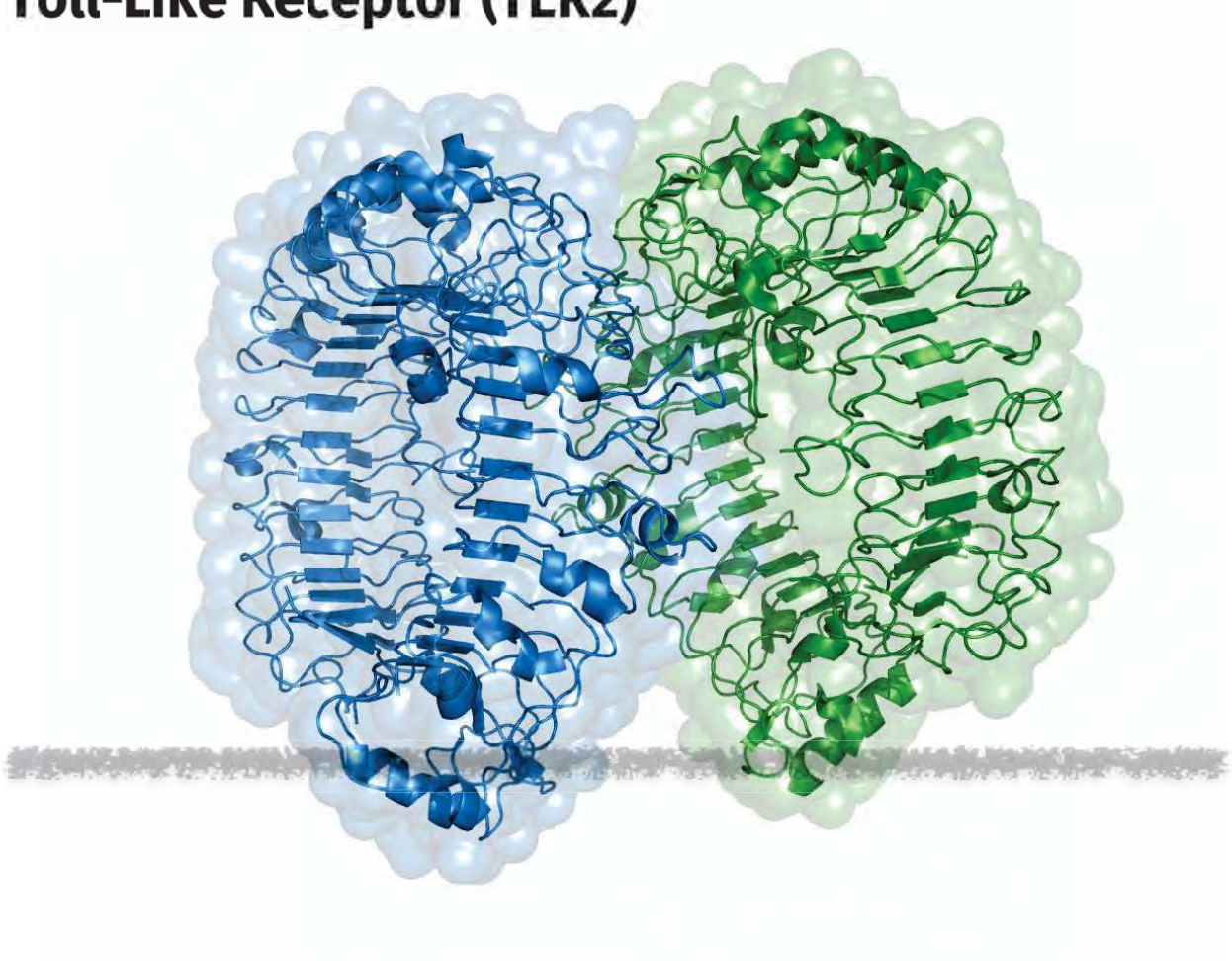

Toll-Like Receptor (TLR2)

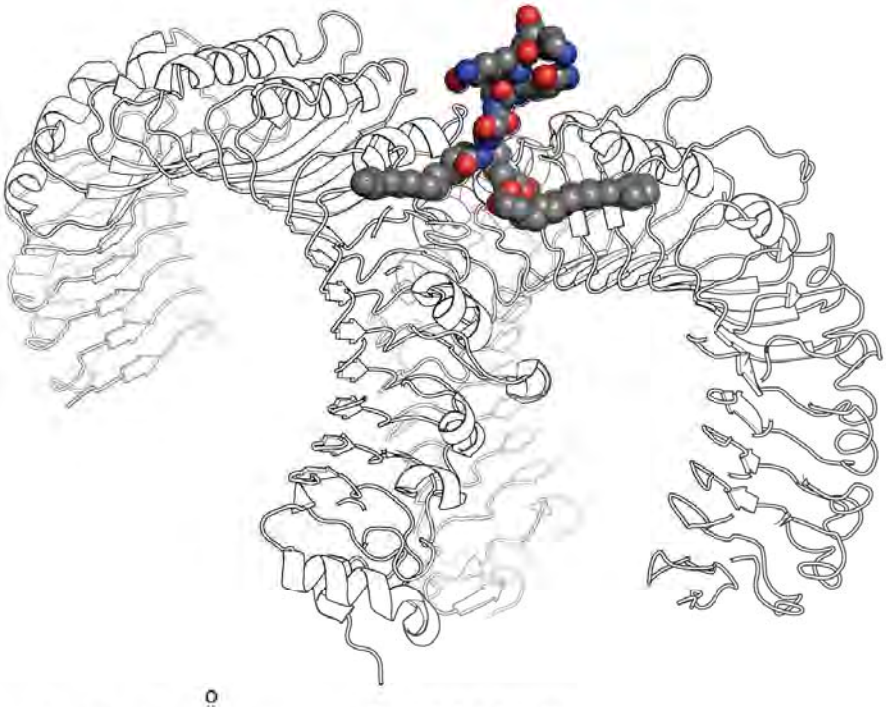

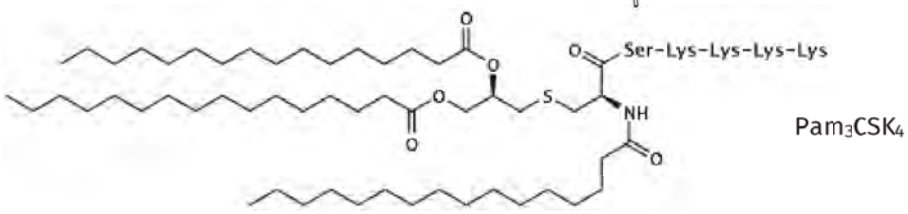

Pam_3CSK_4

Toll-Like Receptor (TLR2)

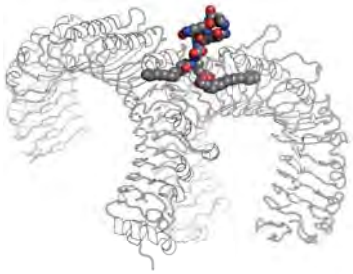

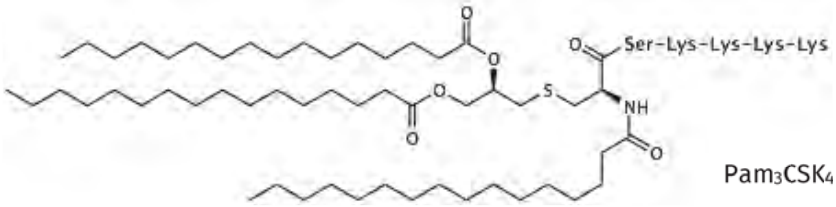

Pam_3CSK_4

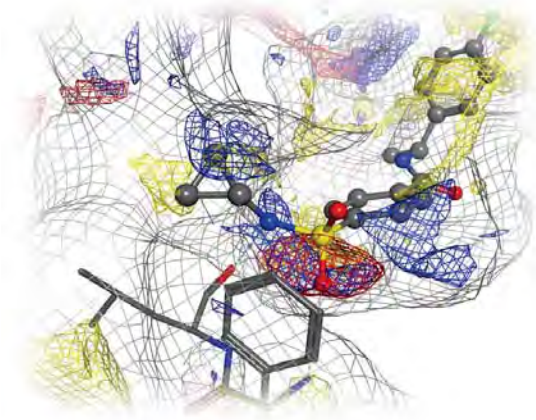

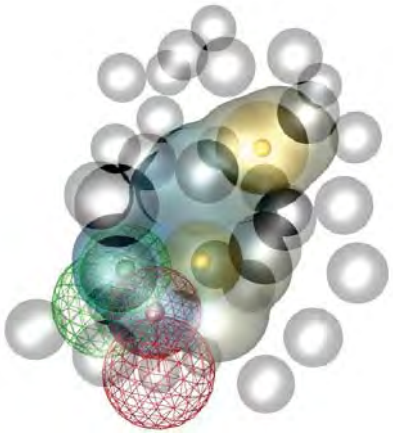

[1] Acute myeloid leukaemia-derived Langerhans-like cells enhance Th1 polarization upon TLR2 engagement, *Pharmacol Res*, 105:44-53, **2016**

[2] Prospective Virtual Screening in a Sparse Data Scenario: Design of Small-Molecule TLR2 Antagonists, ChemMedChem. 9(4):813-22, **2014**

Toll-Like Receptor (TLR2)

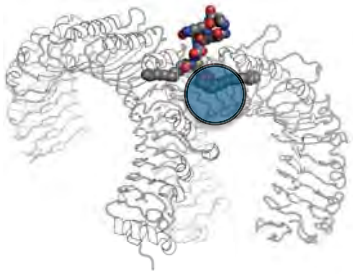

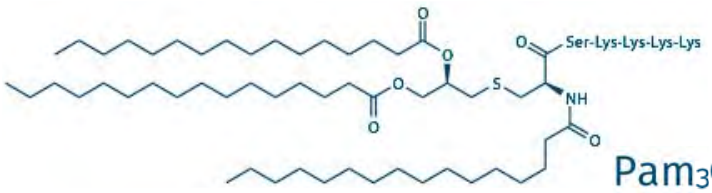

Pam_3CSK_4

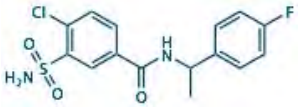

Antagonist 1:
TLR2/1: ~25µM TLR2/6: ~11µM

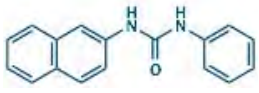

Antagonist 2:
TLR2/1: ~3µM TLR2/6: ~15µM

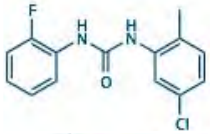

Antagonist 3:
TLR2/1: ~30µM TLR2/6: ~4µM

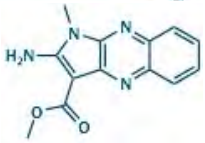

Agonist 1:
still characterized: ~80% Pam_3CSK_4 activity

[1] Prospective Virtual Screening in a Sparse Data Scenario: Design of Small-Molecule TLR2 Antagonists, ChemMedChem. 9(4):813-22, **2014**

[2] Balancing Inflammation: Computational Design of Small-Molecule Toll-like Receptor Modulators, *Trends Pharmacol Sci*, 38,(2): 155–168, **2017**

CU-CPT22 binds differently

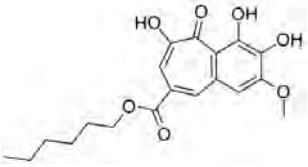

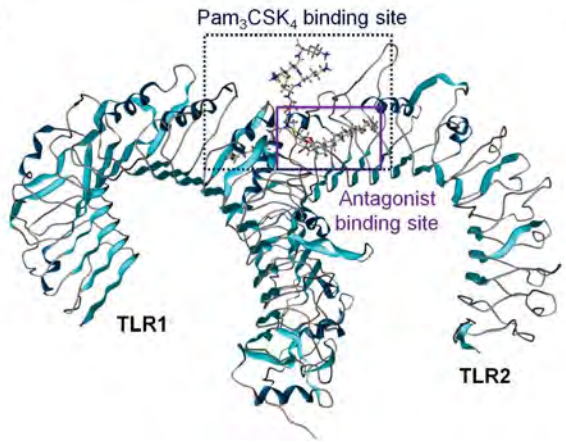

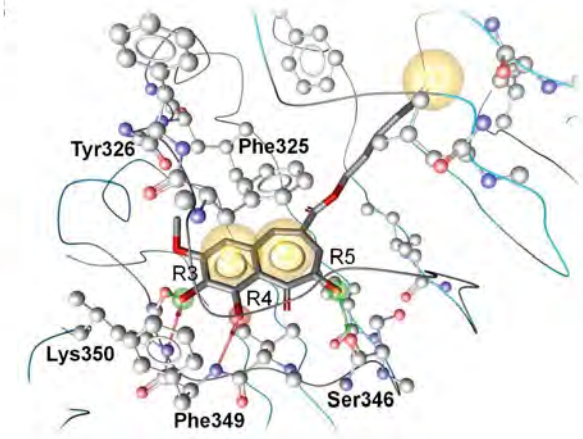

[1] Acute myeloid leukaemia-derived Langerhans-like cells enhance Th1 polarization upon TLR2 engagement, *Pharmacol Res*, 105:44-53, **2016**

[2] Balancing Inflammation: Computational Design of Small-Molecule Toll-like Receptor Modulators, *Trends Pharmacol Sci*, 38,(2): 155–168, **2017**

CU-CPT22 binds differently

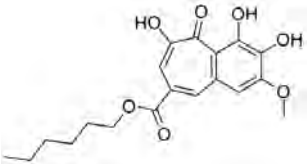

Binding pose by Chen et. al.

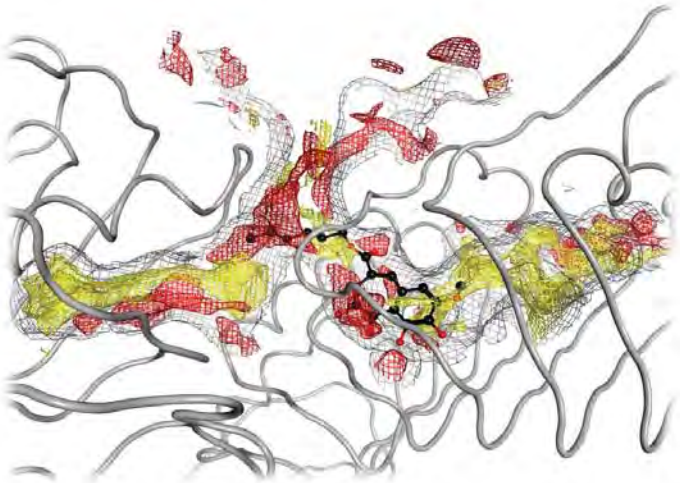

Our proposed binding pose

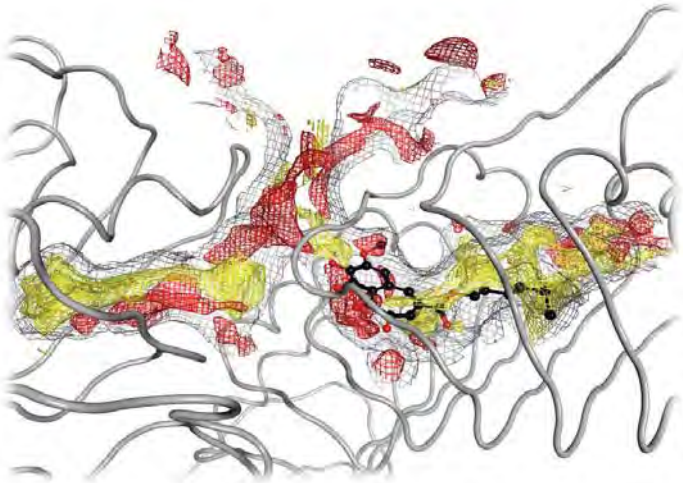

[1] Acute myeloid leukaemia-derived Langerhans-like cells enhance Th1 polarization upon TLR2 engagement, *Pharmacol Res*, 105:44-53, **2016**

[2] Balancing Inflammation: Computational Design of Small-Molecule Toll-like Receptor Modulators, *Trends Pharmacol Sci*, 38,(2): 155–168, **2017**

Pharmacophore Application: TLR2

Virtual Screening
Hit/lead optimization & SAR
Understanding protein function
Design ligands for new pockets

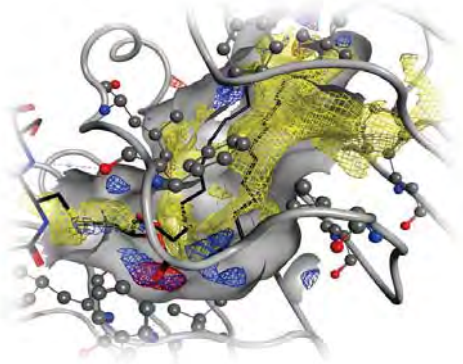

New TLR2 antagonists (structure- and ligand-based):

MIFs for pharmacophore development
3 Mio. screened
51 virtual hits selected
12 biologically active & diverse
(8 antagonists + 4 potential agonists)

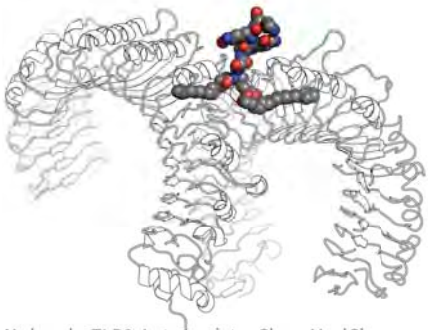

[1] Prospective Virtual Screening in a Sparse Data Scenario: Design of Small-Molecule TLR2 Antagonists, ChemMedChem. 9(4):813-22, 2014

[2] Balancing Inflammation: Computational Design of Small-Molecule Toll-like Receptor Modulators, *Trends Pharmacol Sci*, 38,(2): 155–168, **2017**

Pharmacophore application areas

Virtual Screening ✓
Hit/lead optimization & SAR ✓
Understanding protein function ✓
Design ligands for new pockets ✓

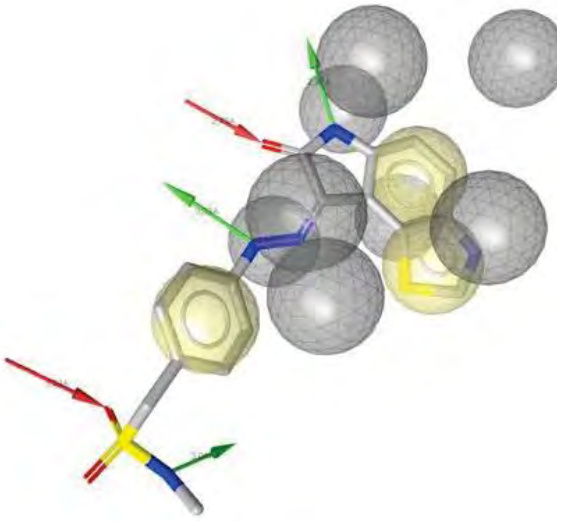

Are available methods consistent?
Scalable? Large screening collections?

Pharmacophore screening (structure-based)

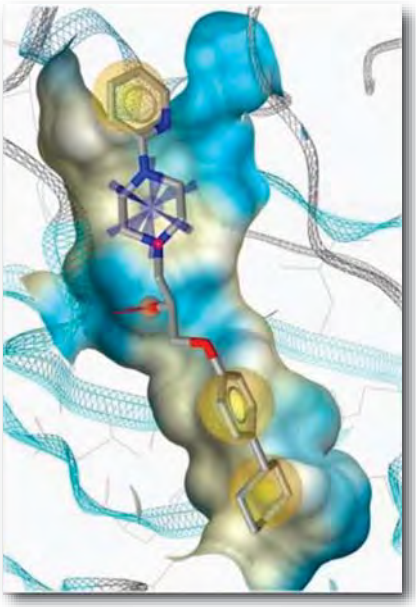

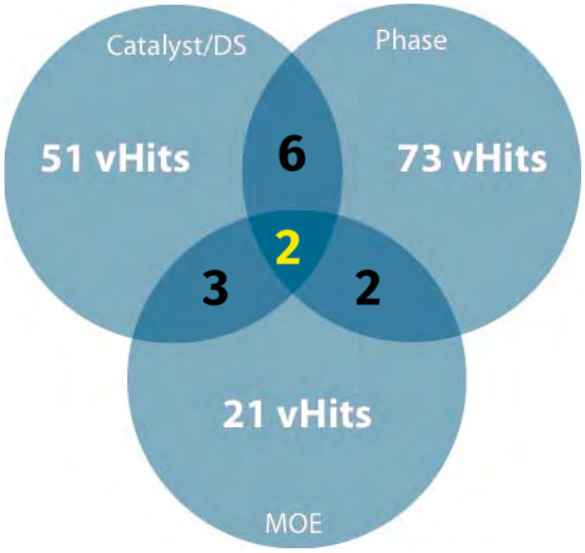

[1] M.Mangold; Master thesis
[2] One Concept, Three Implementations of 3D Pharmacophore-Based Virtual Screening: Distinct Coverage of Chemical Search Space JCIM, 50:1241-1247, 2010

Implementation of pharmacophores ...

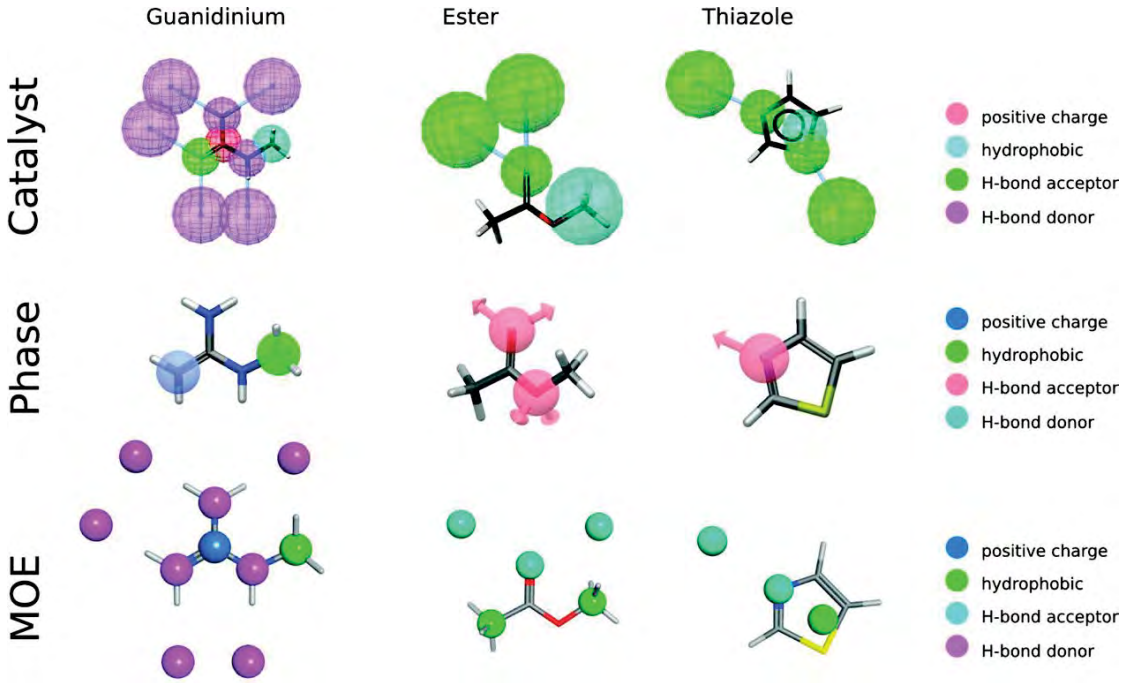

[1] One Concept, three Implementations of 3D pharmacophore-based virtual screening: Distinct coverage of chemical search space. *JCIM*, 50:1241-1247, 2010

Pattern matching vs distance graph

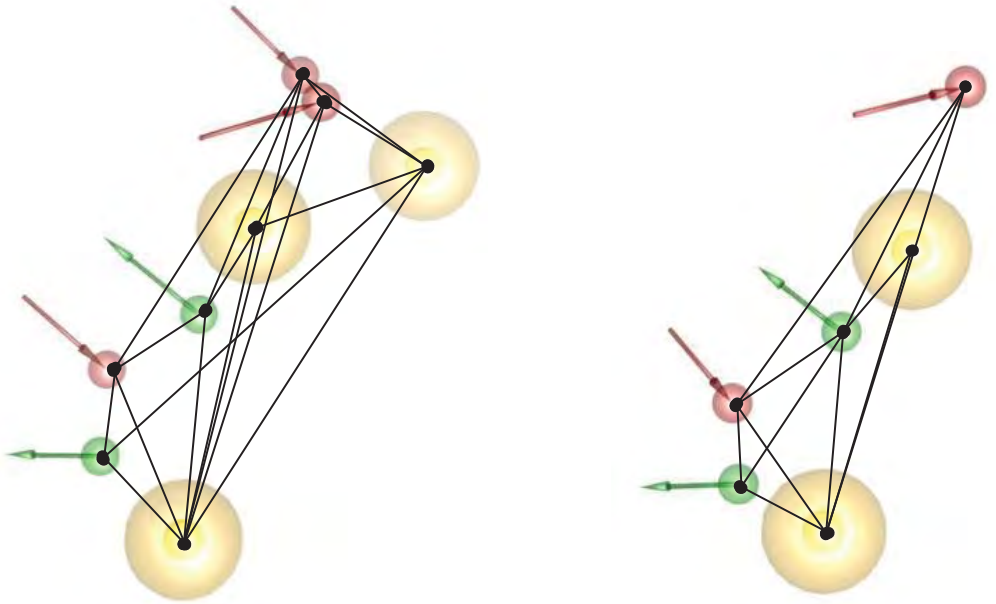

Pattern matching vs distance graph

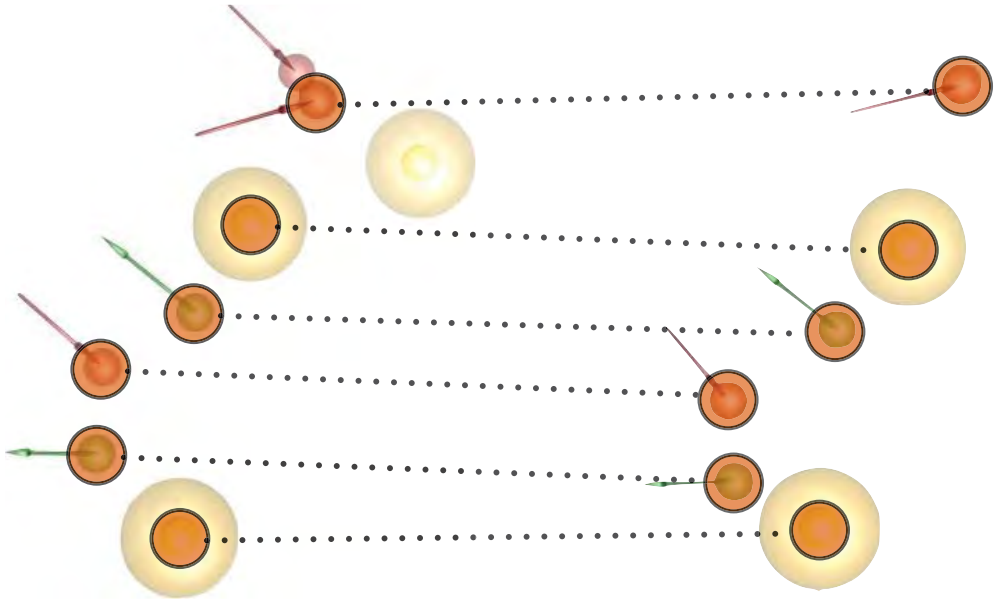

[1] Strategies for 3D pharmacophore-based virtual screening, *Drug Discovery Today: Technologies*, 7(4):e221-e228, 2010

Pattern recognition

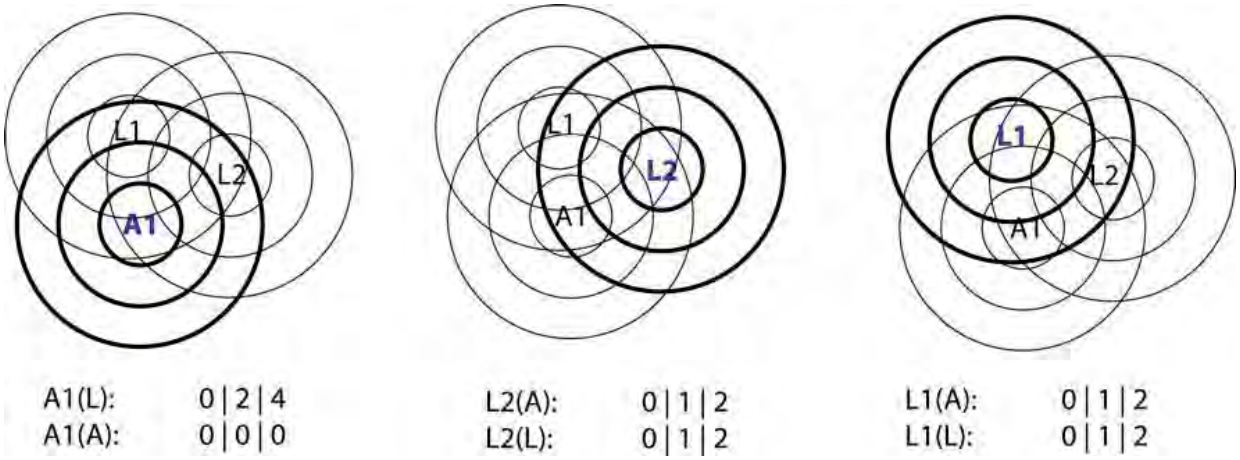

A1(L): 0 | 2 | 4
A1(A): 0 | 0 | 0

L2(A): 0 | 1 | 2
L2(L): 0 | 1 | 2

L1(A): 0 | 1 | 2
L1(L): 0 | 1 | 2

Cost function

$$cost(x,y) = \sum_{shell}\left[weight(shell) * \sum_{type}\left(\min(n_x(shell,type), n_y(shell,type))\right)\right]$$

$n_x(shell,type)$ .... # elements in *shell* of *type* for element *x*
$n_y(shell,type)$ .... # elements in *shell* of *type* for element *y*

$$weight(i_{shell}) = \left(1 - \left(\frac{i_{shell}}{\mathrm{n}}\right)^3\right) * 2\left(1 - \frac{i_{shell}}{\mathrm{n}}\right) * m$$

m .... maximum element count for all shells and all types
n .... maximum shell index
i_{shell} ... shell index

Alignment by pattern recognition

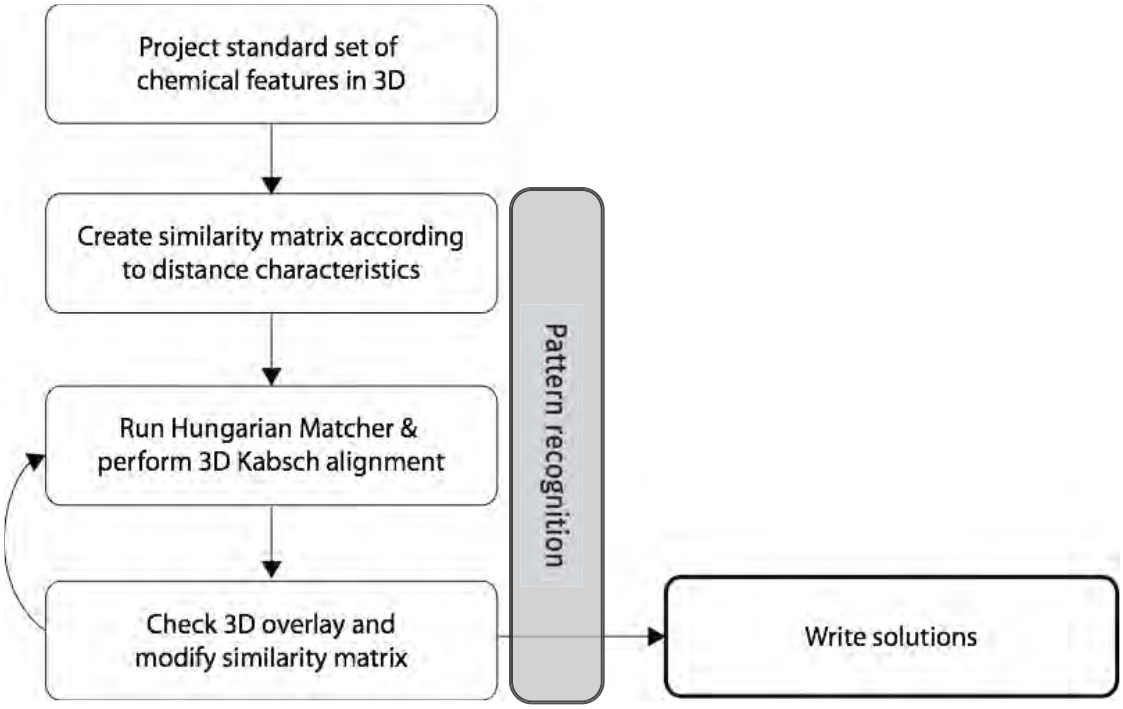

3D Alignment: Phosphodiesterase 5

	1UDT	1TBF	1XP0	1UHO	1UDU	1XOZ
1UDT	-	0,7	0,9	0,3	2,3	2,5
1TBF	0,7	-	0,4	0,7	2,7	3,1
1XP0	0,8	0,4	-	0,8	2,6	--
1UHO	0,3	0,7	0,7	-	2,3	4,5
1UDU	2,2	2,6	2,5	1,7	-	1
1XOZ	2,6	2,9	--	4,5	1	-

Sildenafil

Tadalafil

Vardenafil

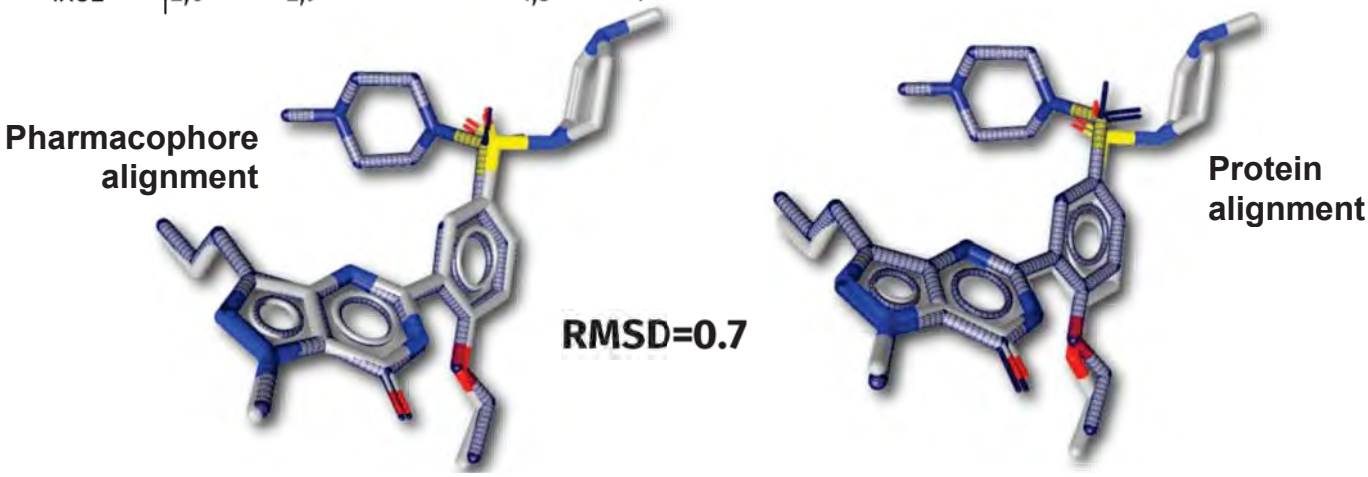

Virtual screening

The tolerance challenge: Accuracy vs ‘fuzziness’

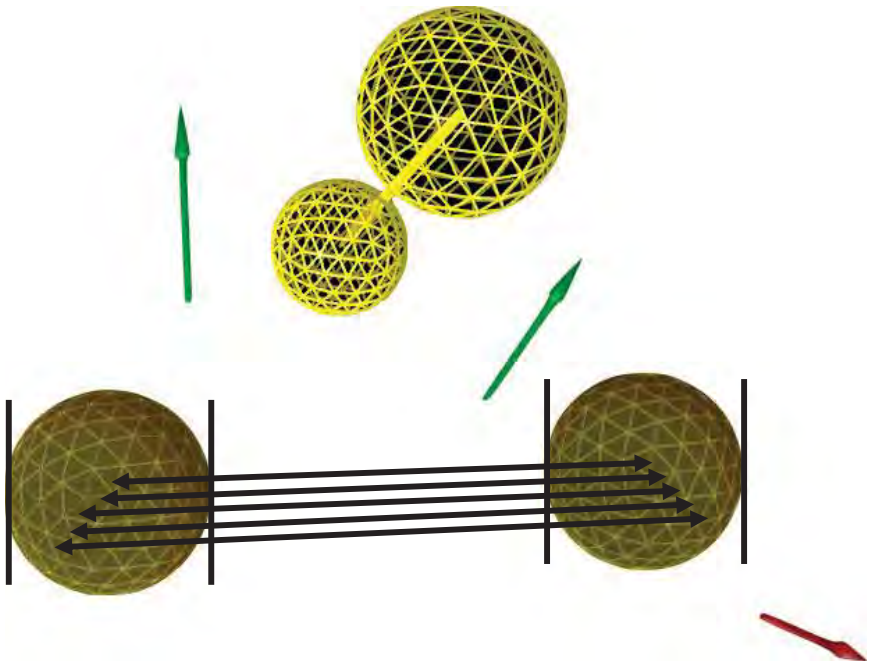

The tolerance challenge: Accuracy vs ‘fuzziness’

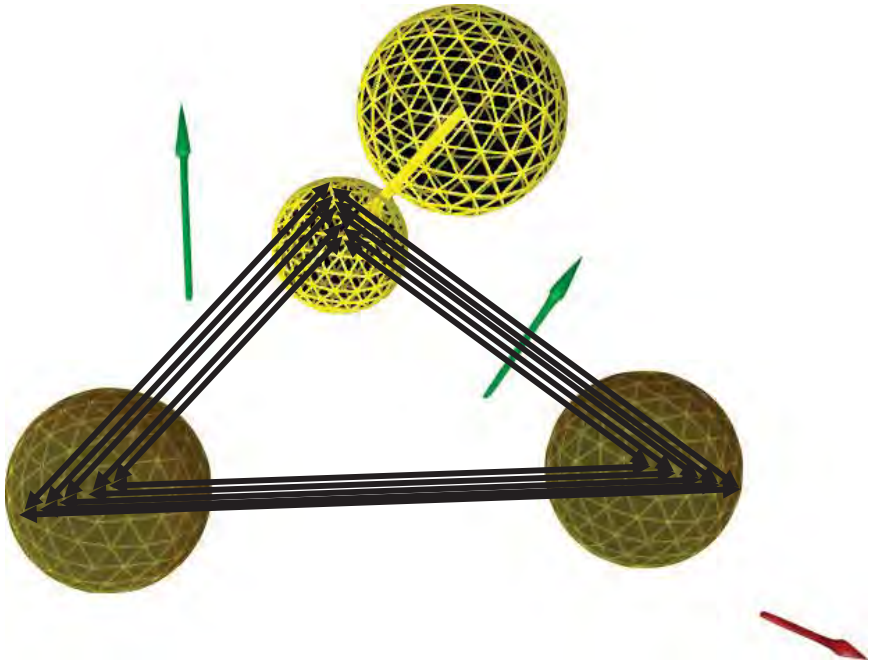

Assessing results: Will accuracy turn into better virtual screening results?

Compared different ligand-based modeling techniques for:

- Alpha1A receptor antagonists
- 5HT2A receptor antagonists
- D2 receptor antagonists
- M1 receptor antagonists

5448 J. Med. Chem. 2005, 48, 5448–5465

Virtual Screening of Biogenic Amine-Binding G-Protein Coupled Receptors: Comparative Evaluation of Protein- and Ligand-Based Virtual Screening Protocols

Andreas Evers,* Gerhard Hessler, Hans Matter, and Thomas Klabunde

Aventis Pharma Deutschland GmbH, Ein Unternehmen der Aventis Gruppe, Chemical Sciences, Drug Design, 65926 Frankfurt am Main, Germany

Received January 31, 2005

In this paper, we compare protein- and ligand-based virtual screening techniques for identifying the ligands of four biogenic amine-binding G-protein coupled receptors (GPCRs). For the screening of the virtual compound libraries, we used (1) molecular docking into GPCR homology models, (2) ligand-based pharmacophore and Feature Tree models, (3) three-dimensional (3D)-similarity searches, and (4) statistical methods (partial least squares (PLS) and partial least squares discriminant analysis (PLS-DA) models) based on two-dimensional (2D) molecular descriptors. The comparison of the different methods in retrieving known antagonists from virtual libraries shows that in our study the ligand-based pharmacophore, Feature Tree-, and 2D quantitative structure−activity relationship (QSAR)-based screening techniques provide enrichment factors that are higher than those provided by molecular docking into the GPCR homology models. Nevertheless, the hit rates achieved when docking with GOLD and ranking the ligands with GoldScore (up to 60% among the top-ranked 1% of the screened databases) are still satisfying. These results suggest that docking into GPCR homology models can be a useful approach for lead finding by virtual screening when either [illegible]

Study published by Evers et al. @ Sanofi Aventis [J. Med. Chem.; 48(17):5448-65, 2005]

Average true positive rate

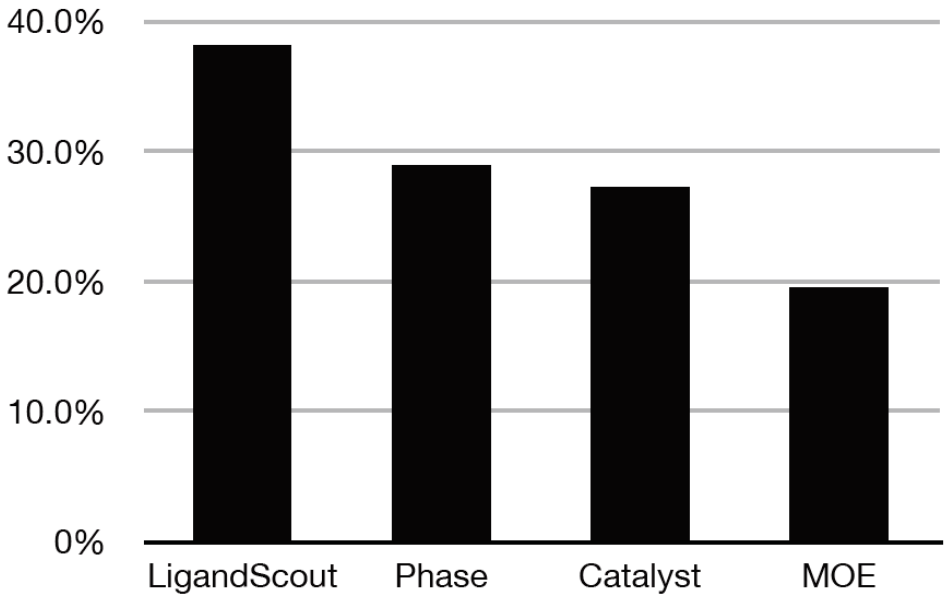

Fraction of true positives in the virtual hit list averaged over all four targets.

‚Dynamic' pharmacophores from molecular dynamics simulations

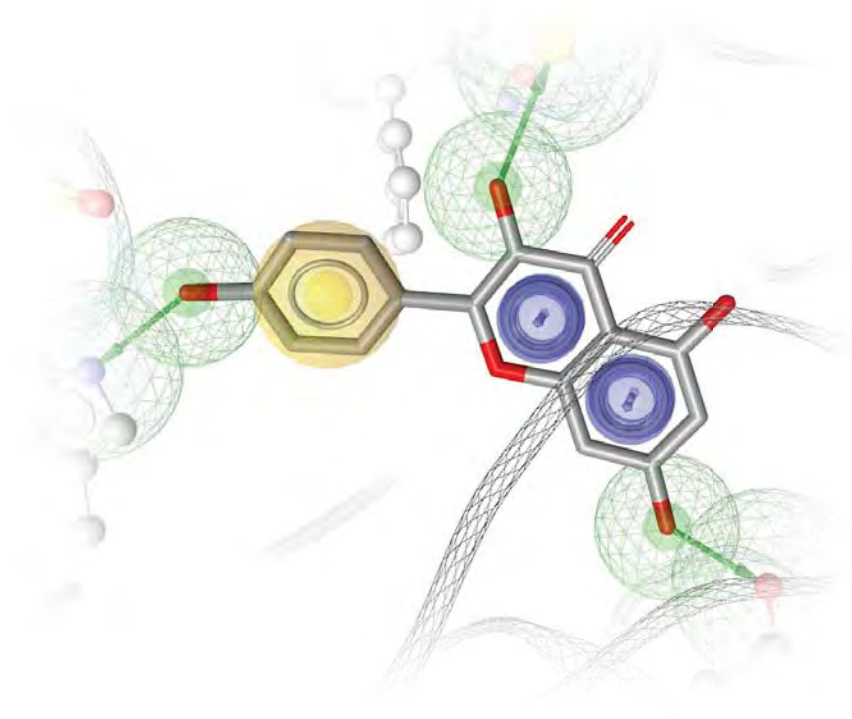

Static view

‚Dynamic' pharmacophores from molecular dynamics simulations

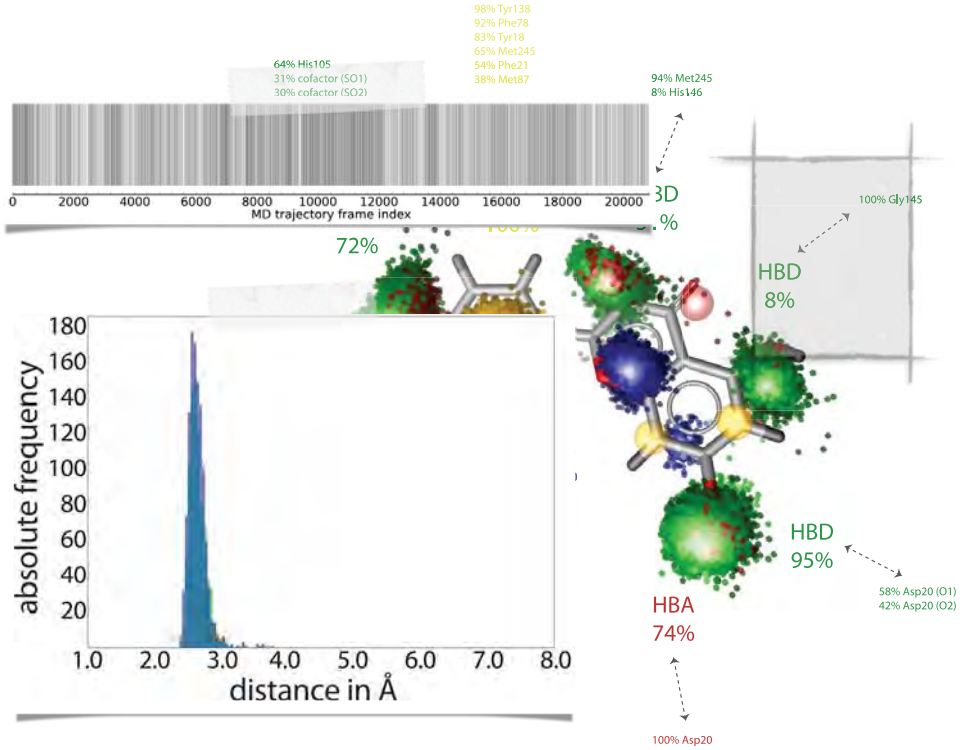

The impact of molecular dynamics on drug design: applications for the characterization of ligand-macromolecule complexes, Drug Discov Today, 120:686-702, 2015.

Summary

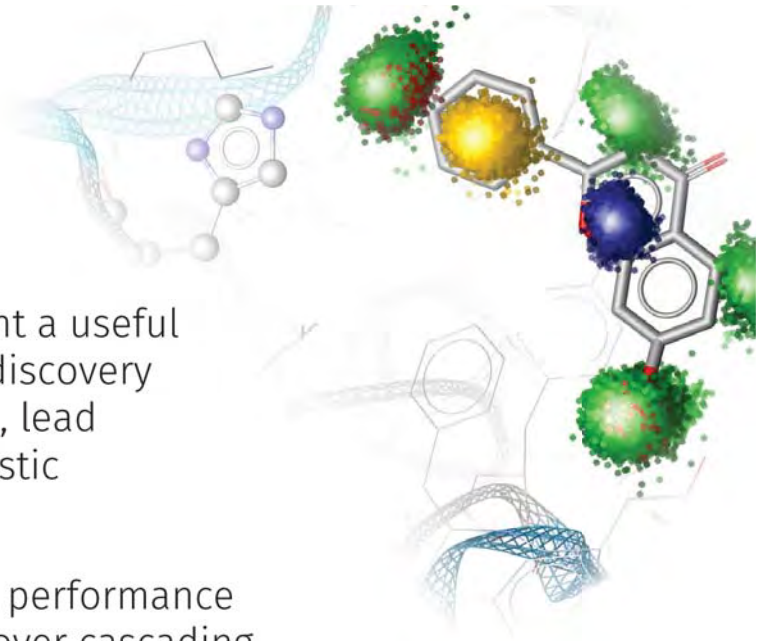

3D pharmacophores represent a useful concept for in silico drug discovery applicable to hit discovery, lead optimization and mechanistic understanding

Pattern recognition provides performance and accuracy advantages over cascading n-point pharmacophore screening algorithms

New technology: **Dynophores** based on molecular dynamics simulations. Adresses the need for fuzziness while maintaining accuracy